PTEP

Prog. Theor. Exp. Phys. **2012**, 03C003 (11 pages)
DOI: 10.1093/ptep/pts064

BigRIPS separator and ZeroDegree spectrometer at RIKEN RI Beam Factory

Toshiyuki Kubo[1,*], Daisuke Kameda[1], Hiroshi Suzuki[1], Naoki Fukuda[1], Hiroyuki Takeda[1], Yoshiyuki Yanagisawa[1], Masao Ohtake[1], Kensuke Kusaka[1], Koichi Yoshida[1], Naohito Inabe[1], Tetsuya Ohnishi[1], Atsushi Yoshida[1], Kanenobu Tanaka[1], and Yutaka Mizoi[2]

[1]*RIKEN Nishina Center, RIKEN, 2-1 Hirosawa, Wako, Saitama 351-0198, Japan*
[2]*Department of Engineering Science, Osaka Electro-Communication University, 18-8 Hatsucho, Neyagawa, Osaka 572-8530, Japan*
[*]E-mail: kubo@ribf.riken.jp

Received October 7, 2012; Accepted November 6, 2012; Published December 20, 2012

The BigRIPS in-flight separator, which became operational in March 2007 at the RI Beam Factory (RIBF) at RIKEN Nishina Center, has been used to produce a variety of rare-isotope (RI) beams by using in-flight fission as well as projectile fragmentation. Its major features are large ion-optical acceptances and two-stage structure. Excellent performance in particle identification is also an important feature. Efficient RI-beam production based on the in-flight scheme has been made possible by these features of the BigRIPS separator, allowing us to greatly expand the accessible region of exotic nuclei. An RI-beam delivery line following the BigRIPS separator is designed to work as a forward spectrometer, called ZeroDegree. As a major experimental device at RIBF, the ZeroDegree spectrometer has been used for a variety of reaction studies with RI beams. In this paper, we present an overview of the BigRIPS separator and the ZeroDegree spectrometer, emphasizing the capability and potential of the new-generation RI beam facility, RIBF.

1. Introduction

A new-generation rare-isotope (RI) beam facility called the RI Beam Factory (RIBF) [1] became operational in March 2007 at RIKEN Nishina Center, which aims to make significant advances in the study of exotic nuclei far from stability. The new superconducting in-flight separator BigRIPS [2,3] has been a major experimental device at RIBF; it is used for the production of RI beams based on the in-flight separation technique and for research with exotic nuclei. The BigRIPS separator is followed by an RI-beam delivery line, which is designed to work as a forward spectrometer, named ZeroDegree [2,4]. The ZeroDegree spectrometer serves to analyze and identify projectile residues produced in reactions with RI beams. The ZeroDegree spectrometer became operational in November 2008, and has been used for studying the structure and properties of exotic nuclei. Figure 1 shows a schematic layout of the BigRIPS separator and the ZeroDegree spectrometer along with the IRC and SRC cyclotrons [1] and the SHARAQ [5] and SAMURAI [6] spectrometers. Here IRC and SRC stand for Intermediate stage Ring Cyclotron and Superconducting Ring Cyclotron, respectively. The RIBF cyclotrons can accelerate all heavy ions up to approximately 350 MeV/nucleon, including very heavy elements such as uranium. The goal beam intensity is as high as 1 pμA, corresponding to 6×10^{12} particles/s [1].

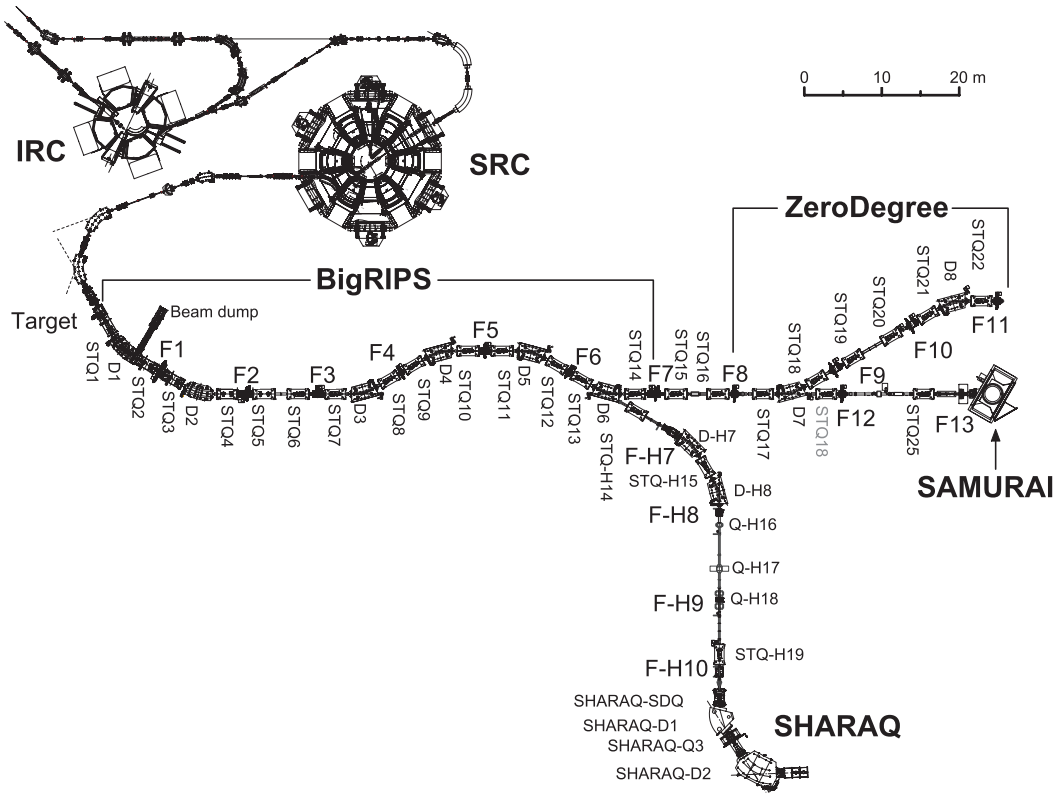

Fig. 1. Schematic layout of the RI Beam Factory (RIBF) at RIKEN Nishina Center.

In the present paper we outline the BigRIPS separator and the ZeroDegree spectrometer in Sects. 2 and 3, respectively, and in Sect. 4 we give an overview of the search for new isotopes and new isomers using a ^{238}U beam and the production of RI beams using a ^{48}Ca beam. The capability and performance of the BigRIPS separator and the potential of RIBF are emphasized; they promise to advance the study of exotic nuclei as well as expand the region of accessible exotic nuclei.

2. BigRIPS separator

The BigRIPS separator is characterized by large ion-optical acceptances, two-stage structure, and excellent particle identification. The large acceptances allow efficient production of RI beams using not only projectile fragmentation of various heavy-ion beams but also in-flight fission of a ^{238}U beam. In-flight fission of fissile beams is known as an excellent mechanism to produce a wide range of neutron-rich exotic nuclei far from stability [7]. The BigRIPS separator has been designed with large acceptances so that the excellent features of in-flight fission can be exploited. Note that fission fragments are produced with much larger angular and momentum spreads, compared with the case of projectile fragmentation. The two-stage structure allows delivery of tagged RI beams and use as a two-stage tandem separator. In delivering tagged RI beams, the BigRIPS separator is operated in a separator–spectrometer mode, in which the first stage of the BigRIPS separator is used to produce and separate RI beams with an energy degrader, while the second stage works as a spectrometer to analyze and identify the RI beams. The momentum resolution of the second stage is designed high enough to identify RI beams without measuring the total kinetic energy, even though fragments are produced in several charge states at our energies. Another energy degrader is placed at the second stage, if the two-stage isotopic separation is needed to further purify the RI beams.

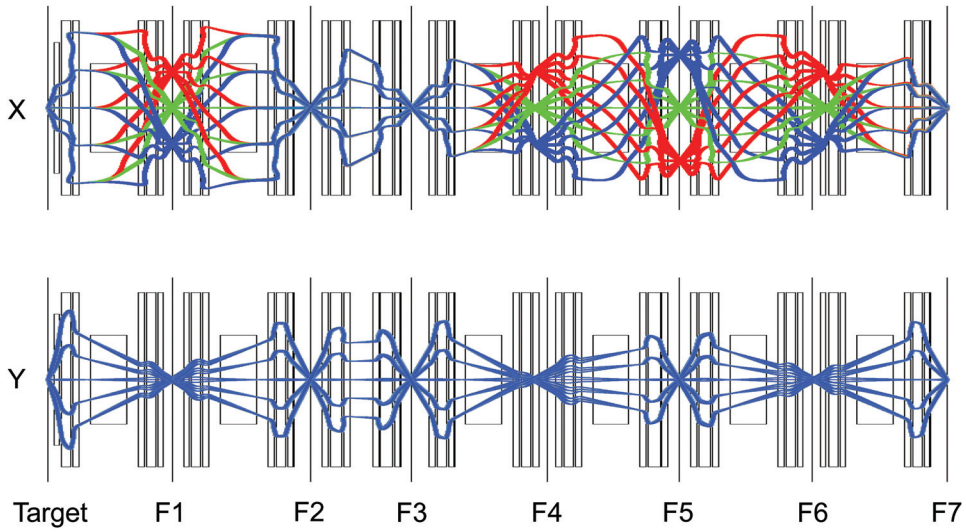

Fig. 2. Standard first-order ion optics of the BigRIPS separator calculated by the COSY INFINITY code: horizontal (upper) and vertical (lower) planes. The foci are denoted by F1–F7.

Table 1. Basic parameters of the BigRIPS separator. $\Delta\theta$ and $\Delta\phi$ indicate the horizontal and vertical angular acceptances, respectively, and δ the momentum acceptance.

$\Delta\theta$[mr]	$\pm$40
$\Delta\phi$[mr]	$\pm$50
δ[%]	$\pm$3
P/ΔP(1st)*	1260
P/ΔP(2nd)**	3420
Max.Bρ[Tm]***	9.5/8.8
Length[Tm]	78.2

*First-order momentum resolution of the first stage, when a beam spot of 1 mm is assumed at the object point (production target).
**First-order momentum resolution of the second stage, when a beam spot of 1 mm is assumed at the object point F3.
***9.5 Tm in the first stage and 8.8 Tm in the second stage.

The BigRIPS separator is composed of fourteen superconducting triplet quadrupoles (STQ) [3,8] with large apertures and high magnetic fields and six room-temperature dipoles with a bending angle of 30 degrees [9]. They are labeled as STQ1–STQ14 and D1–D6 in Fig. 1, respectively. Each STQ consists of three superconducting quadrupoles that are installed in a single cryostat. Except for STQ5 and STQ6, one of the three quadrupoles in the cryostat is equipped with a superconducting sextupole that is superimposed on the inner bore of the quadrupole. STQ1, immediately after the production target, is of an air-core type [10], while the rest of the STQs are superferric quadrupoles that have an iron-dominated structure [8]. There are seven foci along the beam line of the BigRIPS separator, which are indicated as F1–F7. The total length of the BigRIPS separator is 78.2 m, and the length of the second stage (F3 to F7) is 46.6 m. Figure 2 shows the first-order ion optics of the BigRIPS separator, while its basic parameters are summarized in Table 1.

The large acceptances of the BigRIPS separator are achieved by the use of the large-aperture superconducting quadrupoles. This feature allows us to collect fragments with high efficiencies in both in-flight fission and projectile fragmentation, significantly enhancing the capability of expanding

the accessible region of exotic nuclei. The angular acceptances are ±40 mr horizontally and ±50 mr vertically and the momentum acceptance is ±3%, which are comparable with the spreads of fission fragments in our energy domain. The acceptances of the BigRIPS separator allow an approximately 50% efficiency for the collection of fission fragments. The maximum magnetic rigidity ($B\rho$) of the BigRIPS separator is as large as 9.5 Tm in the first stage and 8.8 Tm in the second stage. The $B\rho$ value of the first stage is approximately 19% larger than that of the SRC cyclotron (8 Tm). Thanks to the large $B\rho$ values, a reduction in primary beam energy and/or an increase in target thickness are not needed in producing very neutron-rich RI beams, allowing efficient production of neutron-rich RI beams. The maximum $B\rho$ can be even larger if the ion optics of the BigRIPS separator is adjusted. Although some of the acceptances are lost in this case, a large $B\rho$ allows us to produce very neutron-rich RI beams under optimized conditions.

Another important feature of the BigRIPS separator is the two-stage structure. As seen in Figs. 1 and 2, each stage is designed as a mirror-symmetric achromatic system, in which not only point-to-point focusing but also parallel-to-parallel focusing are attained. The first stage consists of two dipoles (D1 and D2) and four STQs (STQ1–STQ4) located between the production target and the achromatic focus F2, forming a two-bend achromatic system with the momentum-dispersive focus at F1. The second stage consists of four dipoles (D3–D6) and eight STQs (STQ7–STQ14) located between the achromatic foci F3 and F7, forming a four-bend achromatic system with the dispersive foci at F4, F5, and F6. More bends on the second stage allow higher momentum resolution, as listed in Table 1. The two STQs located between F2 and F3 works as a matching section. Fully achromatic conditions are fulfilled at the achromatic foci F2, F3, and F7. The sextupoles installed in the STQs are used to correct second-order chromatic and geometrical aberrations.

The fragments are isotopically separated in flight by a combination of magnetic analysis and energy loss, a technique called momentum-loss achromat [11,12]. Achromatic energy degraders with a wedge shape are inserted into the dispersive foci at F1 and F5 for the isotopic separation. The wedge angle of the achromatic degrader is determined such that the dispersion coefficient is kept the same after slowing down in the degrader, based on energy loss calculations. The achromatic degrader preserves the achromaticity of the system as well.

The matching section between F2 and F3, a telescopic system consisting of two quadrupole triplets, plays a role, for instance, when the ion optics in the second stage should be modified so as to attain higher momentum resolution at F5. In this case the angular magnification at F3, corresponding to the reciprocal of image magnification, is adjusted by using the matching section, so that the loss of angular acceptances can be minimized. Additionally, the matching section allows us to tune the two-stage isotopic separation in a different way. It is possible to adjust the ion optics of the BigRIPS separator such that there is only one focus point between the first and second stages. In such a mode the new focus is located at the mid-point between STQ5 and STQ6. In this case the mass dispersion in each stage, generated by the energy degrader, is added more constructively, allowing different tuning of the two-stage isotopic separation. We can use this mode in order to further improve the purity of RI beams.

The focal-plane chambers located at the foci accommodate various beam-line detectors and devices that are used for the tuning of the BigRIPS separator and for the diagnostics and particle identification of RI beams. Each focus is equipped with two sets of position-sensitive parallel plate avalanche counters (PPAC) [13], in order to measure the position and angle (or trajectory) of RI beams. The tuning of ion optics, such as focusing and achromaticity, and the adjustment of the $B\rho$ setting are performed based on these measurements using the PPAC detectors. The particle identification is

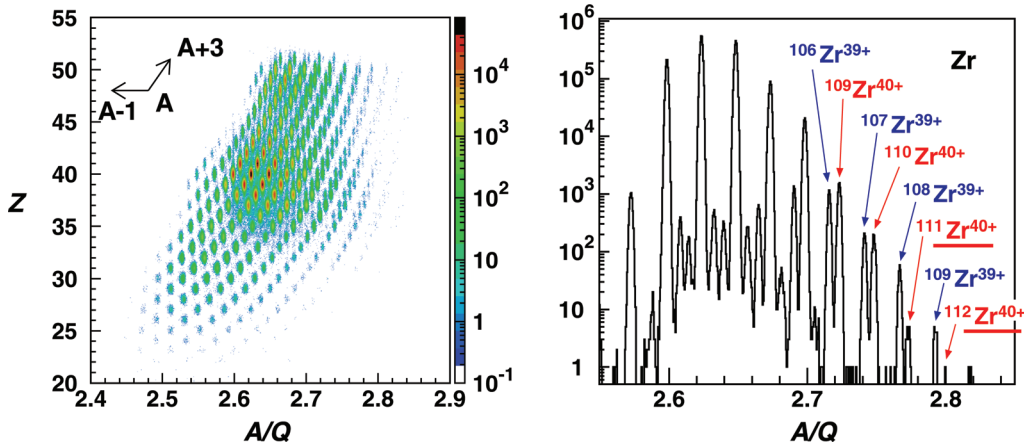

Fig. 3. (Left) Z versus A/Q plot for fission fragments produced in the $^{238}\mathrm{U} + \mathrm{Be}$ (2.9 mm) reaction at 345 MeV/nucleon. (Right) A/Q spectrum of Zr isotopes produced in the same reaction. The $^{111}\mathrm{Zr}^{40+}$ and $^{112}\mathrm{Zr}^{40+}$ isotopes, indicated by an underline, are new isotopes that we identified.

performed on the second stage of the BigRIPS separator, where measurement under low-background conditions is possible. The particle-identification scheme is based on the TOF–$B\rho$–ΔE method, in which the time of flight (TOF), the magnetic rigidity ($B\rho$), and the energy loss (ΔE) of fragments are measured with beam-line detectors to deduce the mass-to-charge ratio (A/Q) and the atomic number (Z) of fragments. The ΔE measurement is made at F7 by using a multi-sampling ionization chamber (MUSIC) [14] or a stack of silicon detectors, while the TOF is measured between two thin plastic scintillation counters placed at F3 and F7. The $B\rho$ measurement is made by trajectory reconstruction from the positions and angles of fragments measured at F3 and F5 by using the PPAC detectors. The $B\rho$ measurement is also made similarly in the second half of the second stage by using the PPAC detectors at F5 and F7. First-order ion-optical transfer maps obtained experimentally and higher-order transfer maps determined empirically are used for the trajectory reconstruction.

A twofold $B\rho$ measurement is needed to deduce the A/Q value of fragments in combination with the TOF measurement, because the fragments are slowed down in the energy degrader and the PPAC detectors at F5. The fragment velocities before and after F5 are determined from the TOF and twofold $B\rho$ measurements. The particle identification is confirmed by detecting delayed γ-rays emitted from short-lived isomeric states of some fragment by using germanium detectors at F7 or another focal plane downstream [15,16]. The observation of characteristic isomeric γ-rays allows unambiguous isotope identification. This technique is called isomer tagging [17]. More details of the particle identification are described in Refs. [15] and [16].

The trajectory reconstruction improves the resolution in the $B\rho$ determination significantly, allowing excellent resolution in the particle identification. Figure 3 shows an example of the particle identification for fission fragments produced in the $^{238}\mathrm{U} + \mathrm{Be}$ reaction at 345 MeV/nucleon. The fully-stripped and hydrogen-like peaks are clearly resolved as seen in the A/Q spectrum, demonstrating the high particle-identification performance of the BigRIPS separator. The achieved r.m.s. A/Q resolution is as good as 3.5×10^{-4} (relative value). In the case of neutron-rich fragments, a hydrogen-like isotope with atomic number Z and mass number A–3 and a fully-stripped isotope with atomic number Z and mass number A have very close A/Q values, appearing at very similar positions in the Z versus A/Q plot and the A/Q spectrum. Excellent A/Q resolution is indispensable for resolving these two peaks, allowing unambiguous particle identification.

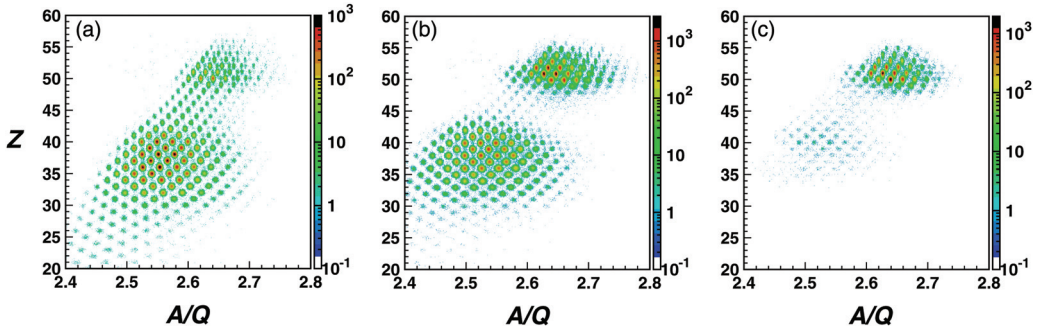

Fig. 4. Z versus A/Q plots for fission fragments that are produced in the reaction ^{238}U + Pb (1.5 mm) at 345 MeV/nucleon. The left (a), middle (b), and right (c) panels correspond to isotope separation with no energy degraders ($B\rho$ analysis only), with a degrader at F1 (3 mm Al), and with degraders at both F1 (3 mm Al) and F5 (1.8 mm Al), respectively. The right panel (c) corresponds to two-stage separation. The $B\rho$ setting of the BigRIPS separator is tuned for ^{140}Te^{52+}.

Figure 4 shows an example that demonstrates the two-stage isotope separation in the BigRIPS separator. 2D particle-identification plots for fission fragments, which are produced in the ^{238}U + Pb reaction at 345 MeV/nucleon, are shown for three cases: without any energy degraders, with a degrader at F1, and with a degrader at both F1 and F5. It can be seen in the Z versus A/Q plots that the contaminant events caused by charge states are well removed by the two-stage separation scheme.

The superconducting quadrupoles in the BigRIPS separator have large fringe fields and large iron saturation effects due to their large aperture, short length, and strong magnetic fields. These are a trade-off to achieve the large acceptances and the large maximum $B\rho$. Accordingly, an ion-optical calculation based on detailed magnetic field maps is indispensable for accurately setting the magnetic fields in the BigRIPS separator. Otherwise it is difficult to fulfill even the first-order ion-optical requirements, such as focusing and achromaticity. We precisely measured the field maps as a function of the magnetic field strength to perform a realistic ion-optical calculation including higher-order terms. The COSY INFINITY code [18,19] is used in the ion-optical calculation.

The experimental conditions to produce rare isotopes, such as the thickness of the target and degraders and the $B\rho$ setting of the BigRIPS separator, are optimized on the basis of detailed simulations using the LISE++ code [20,21].

3. ZeroDegree spectrometer

The ZeroDegree spectrometer is designed as a two-bend achromatic system with anti-mirror symmetry, consisting of two dipoles and six STQs, which are indicated as D7–8 and STQ17–22 in Fig. 1, respectively. The foci are labeled as F8–F11. The magnets of the ZeroDegree spectrometer have the same designs as those in the BigRIPS separator. The object point of the ZeroDegree spectrometer is located at F8, where a secondary target is placed. The intermediate foci at F9 and F10 are momentum dispersive, while the final focus at F11 is fully achromatic. The section from F7 to F8, a telescopic system consisting of STQ15 and STQ16, is used as a matching section between the BigRIPS separator and the ZeroDegree spectrometer. For instance, the ion optics in the matching section can be adjusted according to the actual position of the secondary target at F8 and the required spot size and angular spread of RI beams on the target. Furthermore, when RI beams are delivered to the SAMURAI spectrometer, the matching section is tuned such that the beam conditions at F13 can be optimized. Each focus in the ZeroDegree spectrometer has a focal-plane chamber to accommodate various beam-line detectors and devices that have the same designs as those in the BigRIPS separator.

Table 2. Basic parameters of the ZeroDegree spectrometer. See Table 1 for the definitions of $\Delta\theta$, $\Delta\phi$, and δ.

Optics modes		$\Delta\theta$[mr]	$\Delta\phi$[mr]	δ[%]	P/ΔP*	Max.Bρ[Tm]	Length[m]
Achromatic	Large acc.	±45	±30	±3	1240	8.1	36.5
	Medium Res.	±20	±30	±3	2080	9.7	36.5
Dispersive	Medium Res.	±20	±30	±2	4070	9.8	36.5
	High Res.	±15	±15	±1	6410	10.2	36.5

*First-order momentum resolution, when a beam spot of 1 mm is assumed at the object point F8.

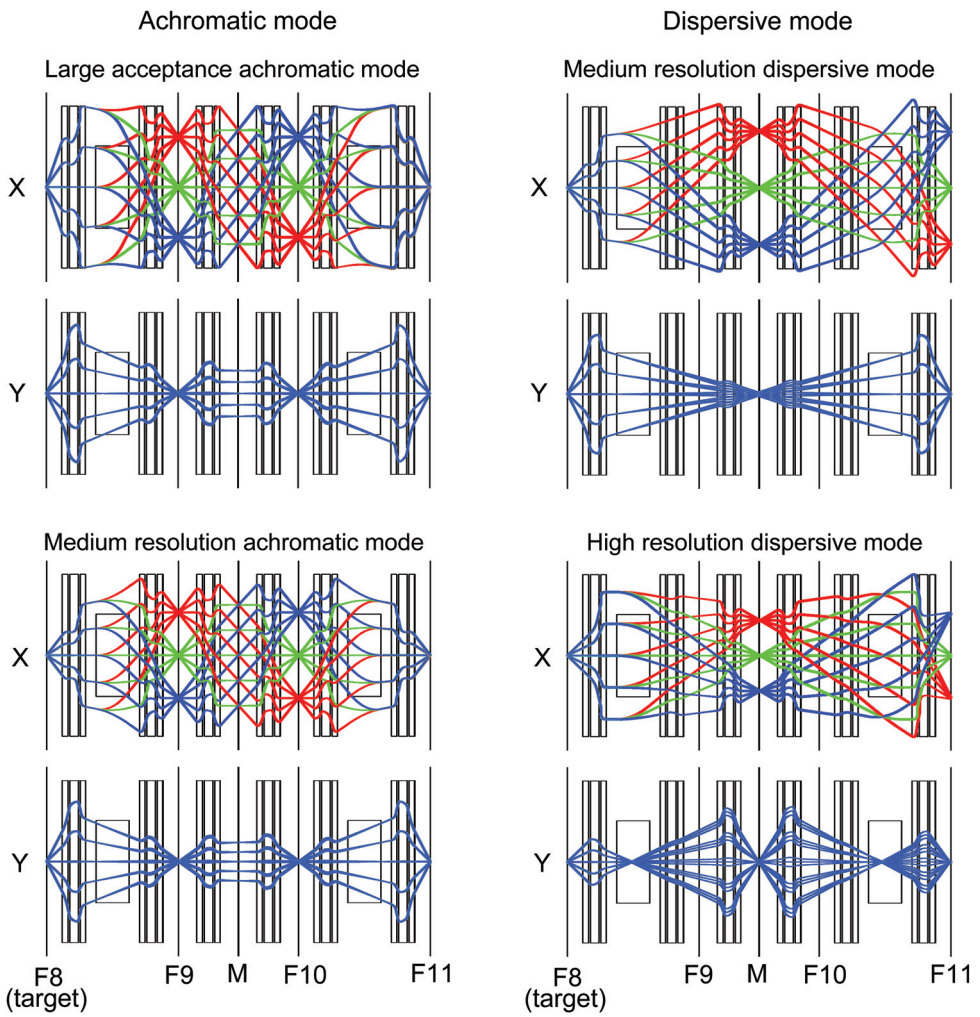

Fig. 5. First-order ion optics of the ZeroDegree spectrometer in four different modes that are calculated using the COSY INFINITY code: horizontal (denoted by X) and vertical (denoted by Y) planes. The foci are denoted by F9–F11 and M. The large acceptance achromatic mode corresponds to the standard optics mode of the spectrometer.

Depending on experimental requirements, it is possible to tune the ZeroDegree spectrometer in different ion-optics modes, including dispersive modes in which the ion optics is tuned such that the final focus at F11 is momentum dispersive. Such flexibility is an important feature of the ZeroDegree spectrometer, helping to optimize the experimental design. Table 2 summarizes the basic parameters of four typical ion-optics modes, including the standard one, called large acceptance achromatic mode. Figure 5 shows their first-order ion optics. Note that there is only one intermediate focus at

the mid-point M in the case of the dispersive modes. The momentum resolution and acceptances vary depending on the ion optics: the better the resolution, the smaller the acceptances, following the principle of ion optics. The standard ion-optics mode is designed with similar acceptances to those of the BigRIPS separator. When RI beams are delivered to an experimental set-up at F11 through the ZeroDegree spectrometer, the ion optics is tuned for the RI-beam delivery mode in which transmission efficiency is optimized. Each STQ in the ZeroDegree spectrometer has one sextupole, allowing correction of second-order chromatic and geometrical aberrations.

In reaction measurements with RI beams, being fixed at 0 degrees, the ZeroDegree spectrometer analyzes and identifies projectile reaction residues in coincidence with γ-rays. A NaI detector array or a germanium detector array, placed by the target at F8, is used to measure the γ-rays emitted from the projectile reaction residues. Particle identification is made based on the TOF–$B\rho$–ΔE method with trajectory reconstruction, similarly to the BigRIPS separator. In the case of the achromatic modes, it is also possible to measure the total kinetic energy (TKE) to be used for additional information for the particle identification. A NaI detector or a CsI detector is employed for the TKE measurement.

4. Expanding the regions of accessible exotic nuclei

Since the commissioning of the BigRIPS separator in March 2007, searches for new isotopes using in-flight fission of 345 MeV/nucleon ^{238}U have been carried out three times, in order to expand the regions of accessible exotic nuclei. During the first run in May 2007, we easily reached the frontiers of known isotopes and could observe the very neutron-rich palladium isotopes ^{125}Pd and ^{126}Pd for the first time, although the uranium beam intensity was as low as 0.007 pnA on average (corresponding to 4×10^7 particles/s) and the total observation time was only one day. The discovery of these new Pd isotopes demonstrated not only the performance of the BigRIPS separator, but also the potential of RIBF. The results were published in Ref. [15] as the first outcome from RIBF.

In November 2008 we revisited the search for new isotopes with ~30 times higher beam intensity than in May 2007. The results demonstrated the overwhelming RI-beam production power at RIBF, as published in Ref. [16]. We ran the measurement at three different settings, each of which is tuned for the production of new neutron-rich isotopes in the $Z \sim 30$, $Z \sim 40$, and $Z \sim 50$ regions, respectively. The net running time was only about four days and the average beam intensity was 0.22 pnA. Figure 6 summarizes the newly discovered isotopes on a nuclear chart. We were able to identify 45 new isotopes over a wide range of very neutron-rich nuclei with Z numbers ranging from 25 to 56. For palladium isotopes, we observed the more neutron-rich isotopes ^{127}Pd and ^{128}Pd, reaching the r-process waiting point at the $N = 82$ neutron magic number. While searching for new isotopes, delayed γ-rays emitted from microsecond isomers were simultaneously detected at the focal plane after ion implantation. We observed a total of 54 isomers, including 18 new isomers in very neutron-rich nuclei, and obtained a wealth of spectroscopic information. This allowed investigation of nuclear isomerism and nuclear structure, such as shape coexistence, nuclear shape, the high-K state, and shell evolution, over a wide range of neutron-rich exotic nuclei [22]. These results also impressively demonstrated the capability of the BigRIPS separator.

In October 2011, we ran the search for new isotopes in the neutron-rich frontiers with $Z \sim 60$. The ^{238}U beam intensity was about 0.2–0.5 pnA. The searched region is indicated in Fig. 6. Delayed γ-rays were also measured simultaneously. Although the data analysis is still in progress, our preliminary results indicate the observation of a number of new isotopes and new isomers in this neutron-rich region.

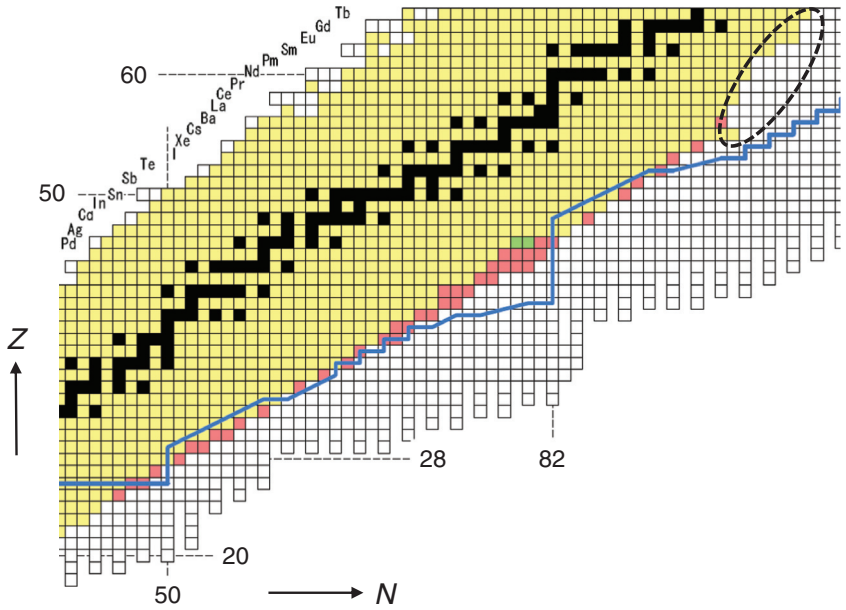

Fig. 6. Nuclear chart showing the new isotopes produced at RIKEN RIBF by using in-flight fission of a ^{238}U beam at 345 MeV/nucleon. Those shown in green and red were discovered in the experiments conducted in May 2007 and November 2008, respectively. The $Z \sim 60$ region that we searched in October 2011 is also indicated with a dashed line. The blue line shows an r-process that is calculated based on the KTUY mass model [16].

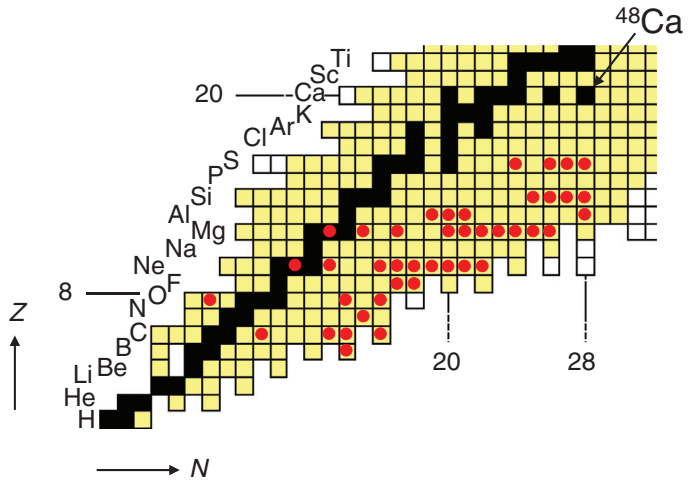

Fig. 7. Nuclear chart showing the rare-isotope beams produced at RIKEN RIBF by using projectile fragmentation of a ^{48}Ca beam at 345 MeV/nucleon. They are indicated by red closed circles.

In December 2008, the ZeroDegree spectrometer was used for the first time for a series of RI-beam experiments, in which 345 MeV/nucleon ^{48}Ca was employed to produce very neutron-rich exotic nuclei, such as ^{22}C, ^{31}Ne, [23] and ^{32}Ne [24]. The RI-beam intensities were approximately 5, 13, and 3 pps/100 pnA for ^{22}C, ^{31}Ne, and ^{32}Ne, respectively. They are orders of magnitude larger than those achieved at the old RIPS facility [25] at RIKEN, demonstrating drastic advances at the new-generation facility. Figure 7 shows the rare isotopes that have been produced by using a ^{48}Ca beam at 345 MeV/nucleon up to now. The intensity of the ^{48}Ca beam has recently reached ∼400 pnA. Most of the very neutron-rich isotopes shown in Fig. 7 have been used for reaction experiments using the

ZeroDegree spectrometer. The nuclear structure of neutron-rich exotic nuclei has been extensively studied by measuring various reactions in inverse kinematics, such as (p, p′), Coulomb excitation, nucleon removal reactions, and secondary fragmentation, in coincidence with γ-rays.

Soon after the new-isotope production experiment in October 2011, the ^{238}U beam intensity was increased to a few pnA. This allowed reaction studies using the ZeroDegree spectrometer for very neutron-rich exotic nuclei produced by in-flight fission. In December 2011, we ran a drip-line search using a ^{124}Xe beam at 345 MeV/nucleon. The ^{124}Xe beam intensity was ∼9 pnA on average. Our analysis indicates the identification of a few new isotopes around the proton drip-line with $Z =$ 41–44.

5. Summary

In the present paper we have presented an overview of the BigRIPS in-flight separator and ZeroDegree spectrometer at RIKEN RIBF. The performance and capability of the BigRIPS separator and the potential of RIBF were emphasized, reviewing the results from the search for new isotopes and new isomers using in-flight fission of a ^{238}U beam at 345 MeV/nucleon. The regions of accessible exotic nuclei are to be greatly expanded towards the drip-line as the beam intensity increases. We may be able to identify 1000 new isotopes or so, if the RIBF goal intensity is achieved for all heavy-ion beams. The scope of RI-beam experiments is being enlarged and the research into exotic nuclei is being promoted by exploiting the capability of this new-generation facility. Other new-generation in-flight RI-beam facilities, such as the Super-FRS at GSI FAIR [26] and the FRIB at MSU [27], are being developed with the same goal.

Acknowledgements

The authors would like to thank the accelerator crew at RIBF who provided primary heavy-ion beams. They also would like to thank Dr Y. Yano, RIKEN Nishina Center, for his support and encouragement.

References

[1] Y. Yano, Nucl. Instrum. Methods Phys. Res., Sect. B **261**, 1009 (2007).
[2] T. Kubo, Nucl. Instrum. Methods Phys. Res., Sect. B **204**, 97 (2003).
[3] T. Kubo et al., IEEE Trans. Appl. Supercond. **17**, 1069 (2007).
[4] Y. Mizoi, T. Kubo, H. Sakurai, K. Kusaka, K. Yoshida, and A. Yoshida, RIKEN Accel. Prog. Rep. **38**, 297 (2005).
[5] T. Uesaka, S. Shimoura, H. Sakai, G. P. A. Berg, K. Nakanishi, Y. Sasamoto, A. Saito, S. Michimasa, T. Kawabata, and T. Kubo, Nucl. Instrum. Methods Phys. Res., Sect. B **266**, 4218 (2008).
[6] K. Yoneda et al., RIKEN Accel. Prog. Rep. **43**, 178 (2010).
[7] M. Bernas et al., Phys. Lett. B **415**, 111 (1997).
[8] K. Kusaka, T. Kubo, Y. Mizoi, K. Yoshida, A. Yoshida, T. Tominaka, Y. Yano, T. Tsuchihashi, N. Kakutani, and K. Sato, IEEE Trans. Appl. Supercond. **14**, 310 (2004).
[9] Y. Yanagisawa, K. Kusaka, T. Kubo, T. Haseyama, Y. Yano, H. Suzuki, and Y. Mizoi, IEEE Trans. Appl. Supercond. **18**, 150 (2008).
[10] K. Kusaka, T. Kubo, Y. Yano, N. Kakutani, K. Ohsemochi, T. Kuriyama, T. Tsuchihashi, and K. Sato, IEEE Trans. Appl. Supercond. **18**, 240 (2008).
[11] J. P. Dufour, R. Del Moral, H. Emmermann, F. Hubert, D. Jean, C. Poinot, M. S. Pravikoff, A. Fleury, H. Delagrange, and K.-H. Schmidt, Nucl. Instrum. Methods Phys. Res., Sect. A **248**, 267 (1986).
[12] K.-H. Schmidt, E. Hanelt, H. Geissel, G. Münzenberg, and J. P. Dufour, Nucl. Instrum. Methods Phys. Res., Sect. A **260**, 287 (1987).
[13] H. Kumagai, A. Ozawa, N. Fukuda, K. Sümmerer, and I. Tanihata, Nucl. Instrum. Methods Phys. Res., Sect. A **470**, 562 (2001).
[14] K. Kimura et al., Nucl. Instrum. Methods Phys. Res., Sect. A **538**, 608 (2005).

[15] T. Ohnishi et al., J. Phys. Soc. Jpn. **77**, 083201 (2008).
[16] T. Ohnishi et al., J. Phys. Soc. Jpn. **79**, 073201 (2010).
[17] R. Grzywacz et al., Phys. Lett. B **355**, 439 (1995).
[18] K. Makino and M. Berz, Nucl. Instrum. Methods Phys. Res., Sect. A **558**, 346 (2006).
[19] K. Makino and M. Berz, COSY INFINITY site, http://www.bt.pa.msu.edu/index_cosy.html, Michigan State University.
[20] O. B. Tarasov and D. Bazin, Nucl. Instrum. Methods Phys. Res., Sect. B **266**, 4657 (2008), and references therein.
[21] O. B. Tarasov and D. Bazin, LISE++ site, http://groups.nscl.msu.edu/lise/lise.html, Michigan State University.
[22] D. Kameda et al., Phys. Rev. C **86**, 054319 (2012).
[23] T. Nakamura et al., Phys. Rev. Lett. **103**, 262501 (2009).
[24] P. Doornenbal et al., Phys. Rev. Lett. **103**, 032501 (2009).
[25] T. Kubo, M. Ishihara, N. Inabe, H. Kumagai, I. Tanihata, K. Yoshida, T. Nakamura, H. Okuno, S. Shimoura, and K. Asahi, Nucl. Instrum. Methods Phys. Res., Sect. B **70**, 309 (1992).
[26] H. Geissel et al., Nucl. Instrum. Methods Phys. Res., Sect. B **204**, 71 (2003).
[27] D. J. Morrissey, J. Phys.: Conf. Ser. **267**, 012001 (2011).